

A numerical study on combined effect of deflector plate, twist angle of blades, and tip speed ratio on the performance of Savonius Hydrokinetic Turbine

Souvik Samadder¹ and B. B. Arora²

¹PG Student, Department of Mechanical Engineering, Delhi Technological University, Delhi, India

²Professor, Department of Mechanical Engineering, Delhi Technological University, Delhi, India

Abstract

Savonius Hydrokinetic Turbine (SHT) is a small-scale renewable energy source that is a sustainable solution for remote areas and rural electrification. The current research work establishes a numerical study on combined effect of deflector plate (no deflector, deflector at 90°, deflector at 45°), twist angle of blades (0°, 12.5°, 25°), and tip speed ratio (0.5 to 1.5) on the performance of turbine in terms of coefficient of power (C_p) using CFD simulation considering a realizable k-ε turbulence model. A total of 99 simulations were performed considering all the above different conditions. To validate the results, simulations were compared with the results of a previous study having no deflector plate. It has been identified that SHT with blade twist angle of 12.5° and deflector plate at 90° produces maximum coefficient of power as 0.364 at a tip speed ratio (TSR) of 0.9 for a 0.5 m/s water velocity. It was observed that C_p increases by an average 15% for SHT having blade twist and deflector plate as compared to SHT without blade twist and deflector plate.

Keywords: *Savonius hydrokinetic turbine, twisted blades, Computational Fluid Dynamics (CFD) simulation, power coefficient, deflector plate, tip speed ratio (TSR)*

1. Introduction

In recent years, the growing global demand for energy, the increasing reliability and cost of fossil fuels, and the unforeseen environmental threats associated with the consumption of fossil fuels have significantly increased the demand for renewable energy [1]. Global electricity demand increased by 81% from 13,152 TWh in 2000 to 23,845 TWh in 2019 and is anticipated to increase by another 58% by 2040 [2]. Global CO₂ emission has increased by 61% in 31 years from 20.5 Gt in 1990 to 33.0 Gt in 2021 [3]. These crises have led researchers and scientists to search for new renewable sources to fulfill energy demand, reduce dependency on fossil fuels, and reduce carbon emissions that harm the environment. Nonetheless, the global renewable energy capacity has shown substantial growth of more than 170% from 1135 GW in 2009 to 3064 GW by the end of 2021 [4]. Hydropower, with an installed capacity of 1230 GW (40 percent), accounted for the highest proportion of worldwide total energy capacity, followed by solar and wind energy, with capacities of 849 GW (28 percent) and 825 GW (27 percent), respectively. The remaining renewable energy sources were estimated at 160 GW (5%), consisting of bioenergy, geothermal, and marine energy [4]. Among renewable energy sources, hydropower is ample, inexpensive, and has maximum potential for electricity production in world [5]. However, conventional largescale hydropower systems are not considered environmentally friendly power generation systems because they need construction of huge water reservoirs or dams, which may severely impact the environment and surrounding ecosystem [6].

Hydrokinetic turbine is a type of hydropower system that produces energy sustainably with less environmental effect. The HKT technology operates similarly to wind turbine, with the distinction of water as operational fluid. It creates power by directly capturing the kinetic energy of water, obviating the need for penstock and dam. [7]. A micro hydrokinetic turbine can act as a small-scale renewable energy source which is a practical and sustainable solution for rural and remote area electrification which are unconnected to the power grid where the load requirement is less than 5kW [8]. We can find streams or canals with low or no water head near rural areas. In such a water flow, installing a traditional hydroelectric plant is impractical. However, a hydrokinetic energy system can utilise the energy of flowing water with low or no head [9].

Hydrokinetic technology can provide an appealing non-polluting source of energy to decrease the necessity of fossil fuels and fulfill the electricity requirement. Hydrokinetic technology is seen as an affordable and environmentally friendly option for electrification in rural and off-grid areas [9]. The design and construction of a traditional Savonius rotor is basic, with an 'S' shape rotor consisting two semi-circular blades [10]. It works on the principle of difference in drag forces that exist between the advancing and returning blades. Savonius hydrokinetic turbine was invented in 1931 by Finnish inventor Sigurd J. Savonius to harness wind energy [11]. In direction of fluid flow, a concave surface is provided on the advancing blade while a convex surface is on the returning blade, the former captures a volume of fluid while later disperses the volume of fluid. The drag force on concave surface is greater than the drag force on the convex surface, which results in a net positive torque. due to blade geometry. Since more the flowing fluid is collected on the concave portion, the pressure on that portion rises, moving the rotor with a net

force and positive net torque. The performance of the rotor can be affected by various parameters such as the number of blades, blade shape, tip speed ratio (TSR), end plate, aspect ratio, overlap ratio, rotor angle, multi-staging, Reynolds number, installation parameters, and augmentation techniques [10,12].

When we compare Savonius hydrokinetic turbine to the conventional hydropower turbine, it begins rotation at a much low water speed. Despite benefits such as high starting torque, low manufacturing costs, an easy construction, low rotational velocity, minimal noise emission, and direction independence of fluid, Savonius hydrokinetic turbines have low efficiency and substantial static torque fluctuation [13,14]. A lot of researches have been conducted in recent years to increase the performance of the Savonius rotor. These studies, which included theoretical, numerical, and experimental work, aimed to improve geometric parameters, blade profiles, and the employment of various augmentation techniques. Savonius rotors having twisted blades have better performance in terms of efficiency, smooth running, and starting ability than semicircular blade rotors [15]. Because of the longer moment arm, a rotor with twisted blades yields more moment than a rotor with a semicircular profile. The highest force operates centrally (curvature center) and vertically in a semi-circular rotor, whereas the maximum force is located at the tip of the blade in the case of a twisted blade due to the twist in the blade. A twisted blade has a greater moment arm as result of these changes, and hence a larger power coefficient value [16]. Saha et al. [17] conducted experiments to investigate the effect of blade geometry on rotor performance, they evaluated the performance of Savonius rotors with semi-circular and twisted blades (twist angle = 12.5°) and it was found that in all circumstances of single, two, and three-stage, the savonius rotor having twist showed improved performance compared to rotor having no twist. To summarise, a two stage system with two blades with a blade twist had the highest coefficient of power, CP=0.31. Kumar et al. [18] performed numerical analysis using CFD to optimize blade twist angle of Savonius hydrokinetic turbine and it was concluded that a Savonius hydrokinetic turbine with 12.5° blade twist angle provides a max. coefficient of power of 0.39, leading to a tip speed ratio (TSR) of 0.9 for water velocity of 2 m/s.

Since the inception of study on the Savonius rotor, researchers have been interested in the tip speed ratio (TSR). The mechanical design of turbine, such as the rotor diameter and number of blades, are important parameters that influence the ideal TSR. If turbine blade rotates at low velocity, they will not be able to capture the majority of the water and will travel through the rotor with less water. However, if the turbine blade rotates at high velocity, it will constantly pass-through turbulent waters. There should be enough time between two rotors passing through the same area for adjacent water to flow in and be harnessed, rather than the used, turbulent water [19]. According to the study of Sheldahl et al. [20], the coefficient of power for two and three blades of savonius wind turbine is optimal for TSR of 0.9 and 0.7, respectively. Zhao et al. [21] found that the maximum power coefficients for a helical Savonius rotor at TSR of 0.81 and 0.55 for two and three-bladed turbines. Kailash et al. [22] performed analysis of modified Savonius turbine and obtained a CP max of 0.15 at tip speed ratio of 0.7. According to Kamoji. et al. [23], at maximum coefficient of power (CPmax), tip speed ratio was determined as 0.69 for a modified Savonius wind turbine. Furthermore, Golecha et al. [24,25] put modified single-stage turbine having deflector plates on the returning blade and two deflector plates on both blades to the test in a water-based environment, and found that the value of TSR at which maximum coefficient of power occurs is 0.82 for single deflector plate and 1.08 for two deflector plates.

Another performance enhancement technique of the Savonius turbine is to utilise deflector, they eventually prevent and divert the fluid flow from striking on the upstream of the returning blade of the rotor. This minimises the drag force on the returning blade, resulting in a large increase in power output [26]. A deflector can be a useful device for enhancing the efficiency in both water and wind applications, however it must be developed and combined with the turbine before it can be practically used. The deflector plate angle may be kept constant in case of hydrokinetic applications since the water flow stream in a river can be fairly anticipated as compared with wind. Air flow, on the other hand, can flow in any direction, complicating design integration [27]. Iio et al. [28] employed a flat plate deflector positioned upstream of a Savonius rotor design to improve savonius rotor's coefficient of power. The analysis illustrated that utilizing a single flat deflector enhanced the CPmax= 0.47 by 80% in comparison to a rotor with no deflector. Golecha [24] performed an experiment to examine how a single flat plate deflector arrangement affects performance of Savonius hydrokinetic turbine, which Kamoji et al. [23] had previously investigated. In their research, they examined eight various deflector configurations upstream of the returning blade and discovered that power coefficient of a modified single-stage Savonius rotor rose by 50% to CPmax=0.21 at TSR=0.82 when deflector plate angle was set to 101° [24].

2. Research Methods

2.1. Performance parameter

The Savonius Turbine's performance is measured by power and torque coefficient as mentioned below:

$$TSR = \frac{\omega R}{V} \quad (1)$$

$$C_{M \text{ average}} = \frac{T}{0.5\rho AV^2 R} \quad (2)$$

$$C_P \text{ average} = \frac{T \omega}{0.5\rho AV^3} = \frac{T}{0.5\rho AV^2 R} \frac{\omega R}{V} = C_{M \text{ average}} \times TSR \quad (3)$$

where ρ = water density [kg/m³], V = free stream velocity [m/s], TSR = tip speed ratio, A = swept area of turbine [m²], ω = rotational speed of turbine [rad/s], R = radius of the turbine [m], T = average moment generated on the turbine [Nm].

2.2. Configuration of deflector plate

Fig. 2 shows the 3 configurations of turbine and deflector plate used for analysis having 2 blades. First configuration design is considered without and deflector plate. Second design consists a deflector plate placed at 90° to the direction of liquid flow. Third design consists a deflector plate placed at 45° to the direction of liquid flow. Further analysis has been done by increasing the twist angle of blades viz. 0° , 12.5° and 25° .

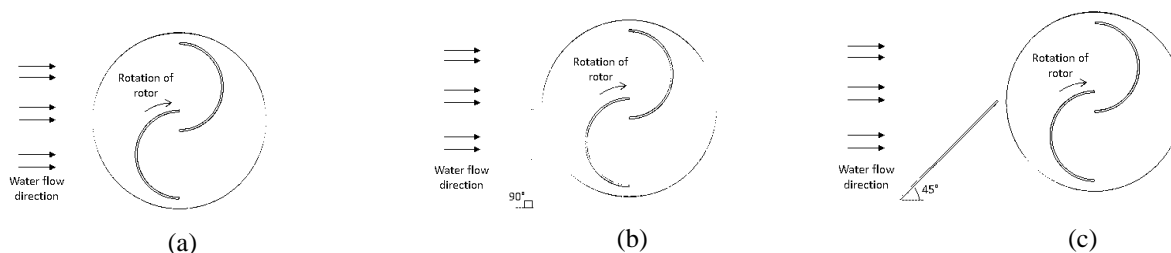


Fig 1: Configurations of turbine and deflector plate arrangement (a) without deflector plate (b) With deflector plate at 90° (c) With deflector plate at 45°

2.3. Design Parameters

A two-blade Savonius HT rotor was designed using SolidWorks considering various parameters viz. number of blades = 2, rotor diameter (D) = 0.16 m, Rotor height (H) = 0.25 m, Aspect ratio (H/D) = 1.5625, Overlap ratio (e) = 0.02 m

Fig. 3 shows show the schematic diagram of Savonius hydrokinetic turbine designed in SolidWoks

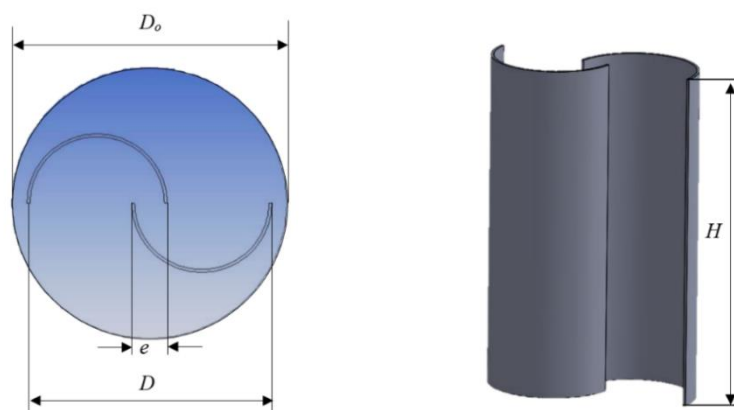


Fig 3:Design parameters of Savonius hydrokinetic turbine

2.4. Rotating Zone

Rotating zone is the volume in the proximity of the turbine blades inside which rotation of blade takes place. Parameters considered for rotating zone are: rotor diameter (D) = 0.18 m and rotor height (H) = 0.27 m

2.5. Stator Zone

Stator zone or open channel flow is the volume where flow of water takes place. Free stream velocity in water channel considered in analysis is 0.5 m/s. Parameters for stator zone are:open channel length = 3 m, open channel height = 0.6 m, open channel width = 0.6 m, and blockage ratio = 13.5

2.6. Boundary Conditions

Table 1 shows the various boundary type and boundary conditions taken into consideration in this study, and also depicted in Fig. 4. The velocity inlet on the left side of the channel is set to free stream velocity of 0.5 m/s. The outflow condition has been established at the extreme right border. The channel's side and bottom walls are designated as slip boundaries. Symmetry is given to the channel's top. Free surface effects aren't taken into account in this analysis because the turbine is thought to run at a depth that minimises the surface impact. The Savonius turbine, which is located inside the rotating zone, has a rotating wall condition (no-slip wall). The angular velocity of rotation zone is taken depending on tip speed ratio. As a result, several simulations are performed with different TSRs and free flow velocity.

Table 1: Boundary conditions for Numerical Analysis

Name	Boundary type	Boundary condition
Inlet	Velocity Inlet	0.5 m/s, uniform flow
Outlet	Outflow	Outflow
Channel side, bottom, and top wall	Free slip wall	Stationary
Turbine	No slip wall	According to TSR

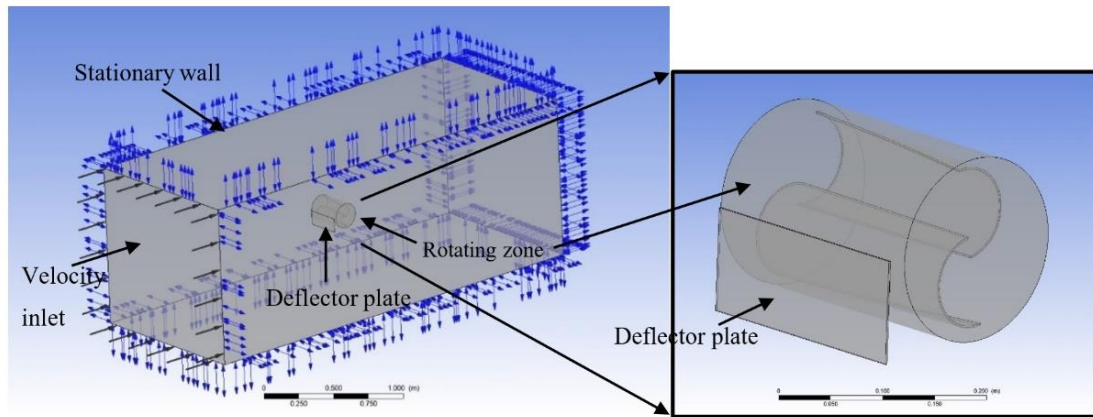


Fig 4: Boundary conditions for CFD analysis

2.7. Meshing

Meshing has been done in Ansys Mesh System. For CFD investigations, a large flow domain is desired, but it must be constrained according to the computational load and the type of the flow issue being handled [29]. Computational subdomain was meshed using non-conformal unstructured lattice with tetrahedral elements. Because the mesh quality has a significant impact on the accuracy of CFD outcomes, an unstructured grid allows greater flexibility for automatic mesh generation in complex geometries. Fig. 5 shows the meshed model for rotor and stator zone of 0° blade twist. Number of elements for rotor zone is 4,62,451 and maximum skewness is 0.79637. Number of elements for rotor zone is 4,64,189 and maximum skewness is 0.79985.

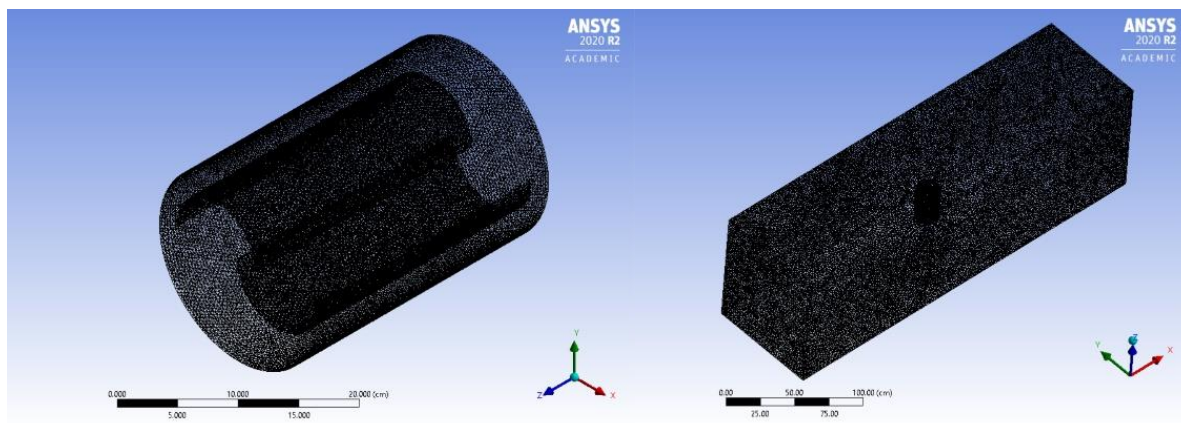


Fig 5: (a) Mesh for Rotor Zone of 0° blade twist (b) Mesh for Stator Zone of 0° blade twist

3. Simulation Procedure

Flow solver used in present study is ANSYS FLUENT, which was utilised to resolve unsteady incompressible Navier-Stokes equations. The Reynolds averaged Navier- Stokes equations are solved using the finite volume approach to represent the flow field. The case with the relevant boundary conditions is specified and solved in order to achieve a numerical solution.

3.1. Turbulence Model

Turbulence must be taken into account while modelling water flow. For modelling turbulence, a variety of models are available, and the model used is determined by the flow shape and Reynolds number. In the research by Mohamed et al. [30] it was suggested that Realizable $k-\epsilon$ turbulence model is better to simulate the rotating behaviour of blades or air foil, flow through the channel, a boundary layer or separated flows. As a result, the Realizable $k-\epsilon$ model was used to represent the rotational motion of

turbine blades in present study. This model includes a novel turbulent viscosity formulation and a new dissipation rate transport equation derived from an exact solution for the transport of mean-square vorticity fluctuations. Furthermore, it does not take into account the anticipated link between the Reynolds stress tensor and the strain rate tensor.

The transport equations for Realizable k- ε model are given as [31]:

$$\frac{\partial}{\partial t}(pk) + \frac{\partial}{\partial x_j}(pk u_j) = \frac{\partial}{\partial x_j} \left[\left(\mu + \frac{\mu_t}{\sigma_k} \right) \frac{\partial k}{\partial x_j} \right] + G_k + G_b - \rho \epsilon - Y_M + S_k \quad (4)$$

$$\frac{\partial}{\partial t}(p\epsilon) + \frac{\partial}{\partial x_j}(p\epsilon u_j) = \frac{\partial}{\partial x_j} \left[\left(\mu + \frac{\mu_t}{\sigma_\epsilon} \right) \frac{\partial \epsilon}{\partial x_j} \right] + \rho G_k S_\epsilon + \rho C_2 \frac{\epsilon^2}{k + \sqrt{\nu} \epsilon} + C_{1\epsilon} \frac{\epsilon}{k} C_3 C_b + S_\epsilon \quad (5)$$

where, k =turbulent kinetic energy; ε = dissipation rate of the turbulent kinetic energy; ρ = density of fluid; u_j = velocity components; x_j = Cartesian coordinate, t = time; μ = viscosity μ_t = turbulent viscosity; σ_k = constant of k-ε turbulence model; G_k = generation of turbulence kinetic energy due to the mean velocity gradients; G_b = generation of turbulence kinetic energy due to buoyancy; Y_M = effect of the changing dilatation in compressible turbulence to the overall dissipation rate.

4. Results and Discussions

A total of 99 simulations were performed in this study for different tip speed ratio (TSR) values varying from 0.5 to 1.5 and for blade twist ranging for 0°, 12.5° and 25° for 3 different deflector plate configurations. Simulation results were achieved for all of the parameter values investigated.

4.1. Velocity Contours

At the blade's tip, a high speed zone has been observed., as shown in Fig 6. Low speed zone (wake zone) is noticed behind rotor blades due to turbine rotation as shown in Fig 6. The flow velocity in the wake zone is substantially reduced. The flow velocity is periodically raised at the higher and lower ends of the wake zone, resulting in a "periodic high speed zone."

Figure 7-9 illustrates, velocity contour plots which depicts the changes in velocity across different places around the SHT having blade twist angle 0°,12.5° and 25° respectively at TSR of 0.7 and also with 3 configurations of deflector plate.

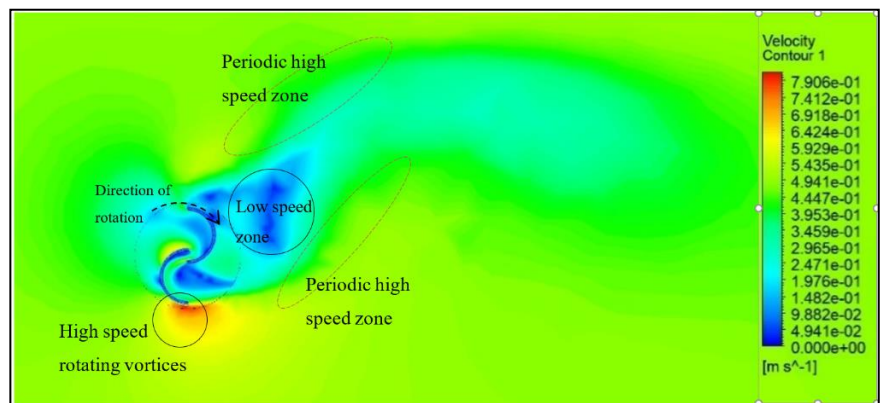


Fig 6: Velocity contours for 0° twist angle at TSR = 0.7 and 0.5 m/s

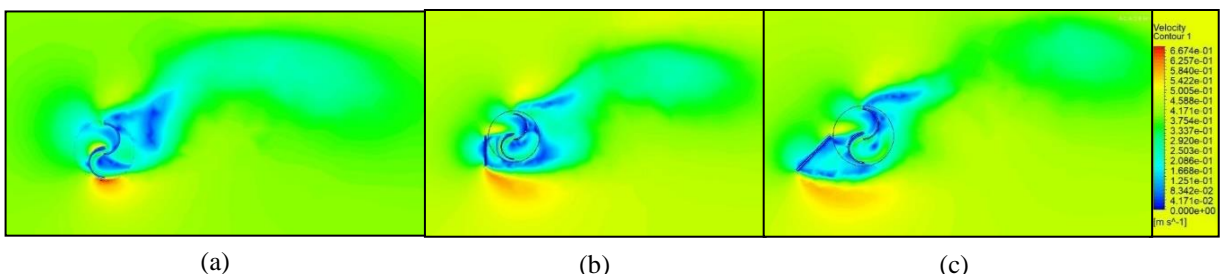


Fig 7: Velocity contours for 0° blade twist angle at TSR = 0.7 (a) without deflector plate (b) With deflector plate at 90° (c) With deflector plate at 45°

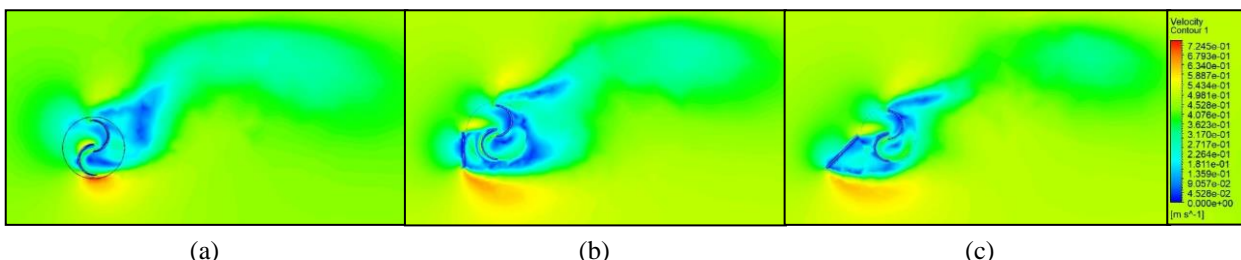


Fig 8: Velocity contours for 12.5° blade twist angle at TSR = 0.7 (a) without deflector plate (b) With deflector plate at 90° (c) With deflector plate at 45°

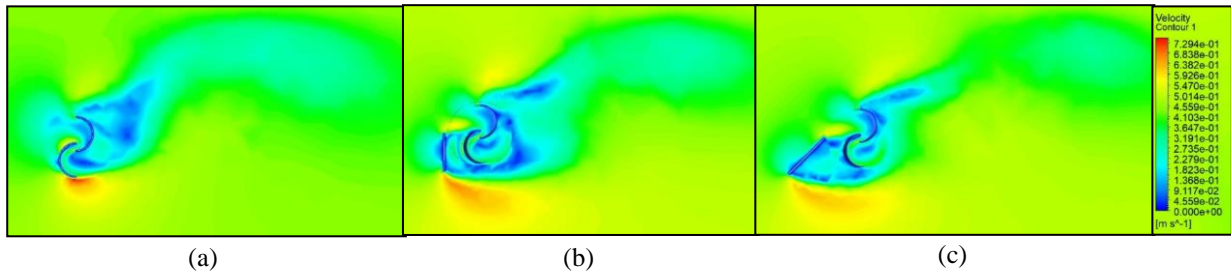


Fig 9: Velocity contours for 25° blade twist angle at TSR = 0.7 (a) without deflector plate (b) With deflector plate at 90° (c) With deflector plate at 45°

4.2. Pressure Contours

Pressure contour plots are used to anticipate pressure differences in various places close to turbine blades in flow domain. Blue and red colours show the minimum and maximum pressure values in pressure contours, respectively. Fig 10 shows that high pressure zone is created near the advancing blade whereas low pressure zone is created near returning blade. Thus, these two pressure zones produce a pressure drop across the rotor and causes the blades to rotate which in turn produces power by energy extraction by the Savonius hydrokinetic turbine from the flowing water.

Fig 11-13 depicts pressure contour of rotor for 0°, 12.5°, 25° twist angle respectively at TSR of 0.9 for 3 different deflector plate configuration and free stream velocity of 0.5 m/s. We can observe that pressure decreases on rotor from upstream to downstream.

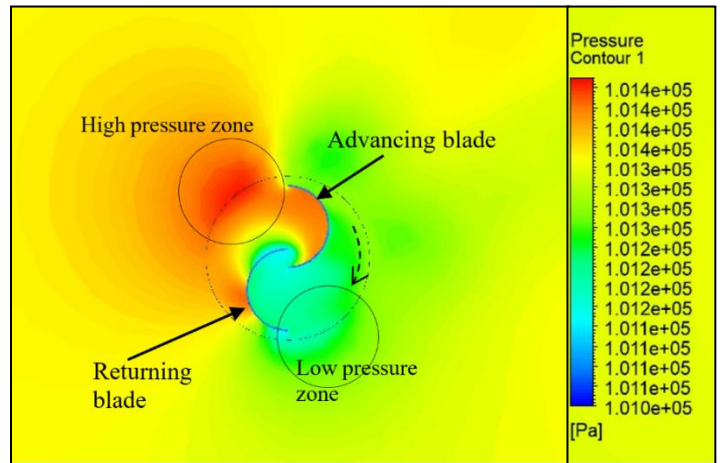


Fig 10: Pressure contours for 0° twist angle at TSR = 0.7 and flow velocity of 0.5 m/s

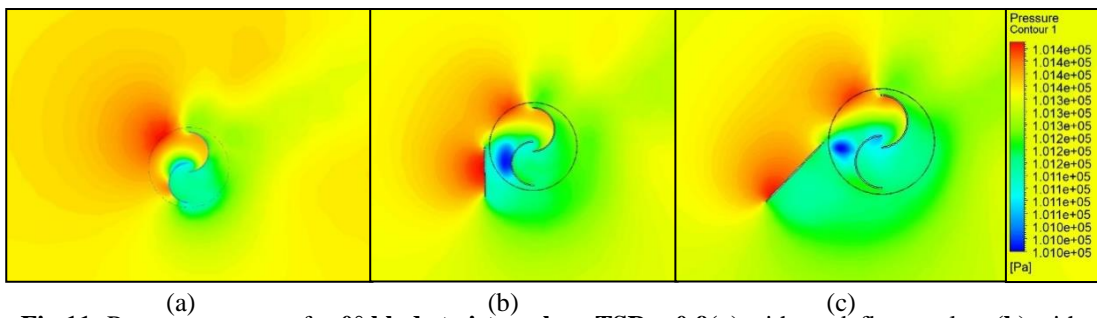


Fig 11: Pressure contours for 0° blade twist angle at TSR = 0.9 (a) without deflector plate (b) with deflector plate at 90° (c) with deflector plate at 45°

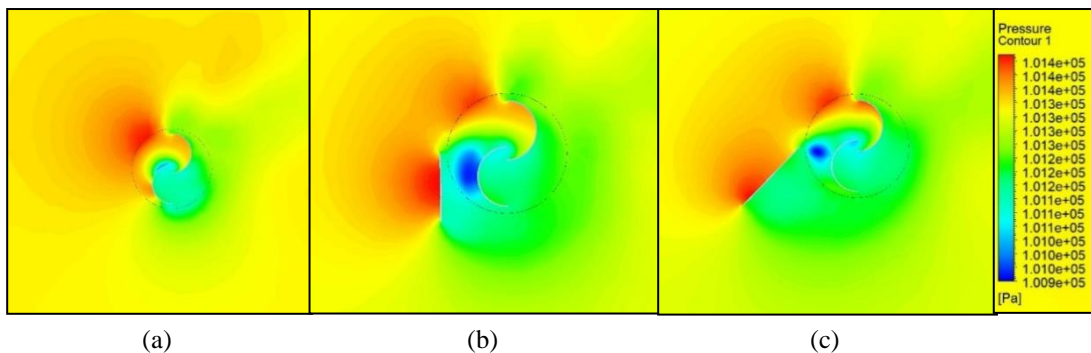


Fig 12: Pressure contours for 12.5° blade twist angle at TSR = 0.9 (a) without deflector plate (b) with deflector plate at 90° (c) with deflector plate at 45°

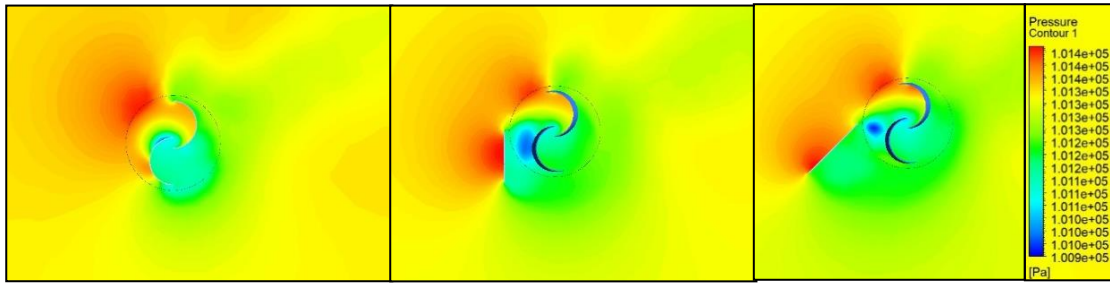


Fig 13: Pressure contours for 25° blade twist angle at $TSR = 0.9$ (a) without deflector plate (b) with deflector plate at 90° (c) with deflector plate at 45°

4.3. Variation of Power Coeff. (C_p) & Torque Coefficient (C_t) w.r.t. TSR

Figure 14 - 15 represents the variation of power coefficient (C_p) and torque coefficient (C_t) with respect to TSR for different values of blade twist angle viz. $12.5^\circ, 25^\circ$ along with 3 configuration of deflector plate.

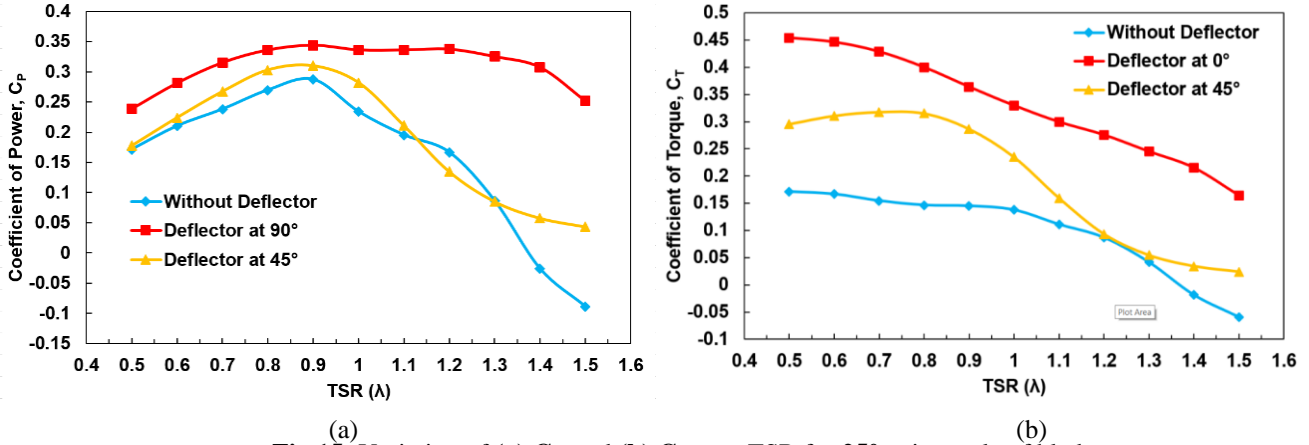
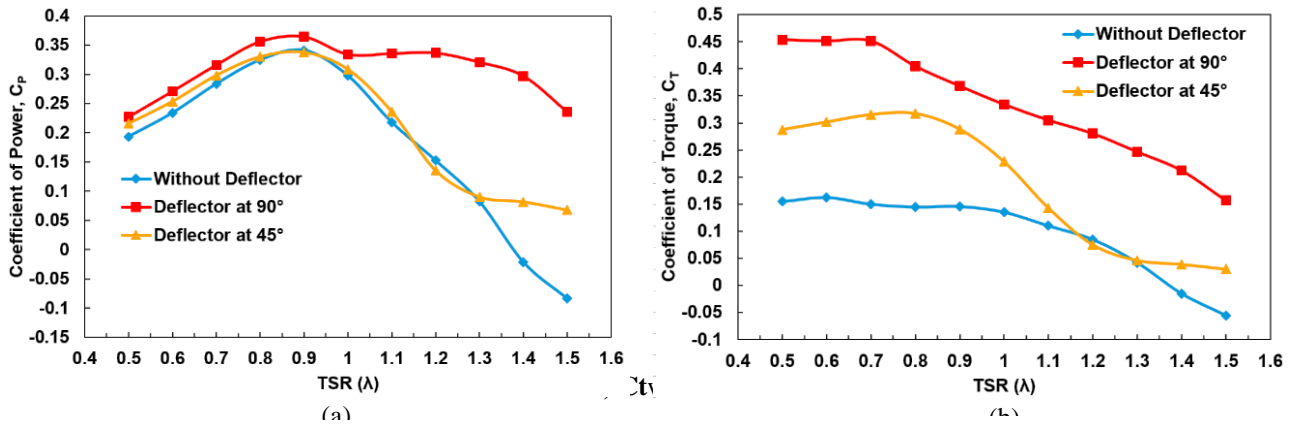


Fig 15: Variation of (a) C_p and (b) C_t w.r.t. TSR for 25° twist angle of blade

Table 2 provides the maximum power coefficient (C_p), and the tip speed ratio that corresponds for different blade twist angles along with deflector configuration.

Blade Twist Angle ($^\circ$)	Deflector plate configuration	Maximum Coefficient of Power ($C_{p \max}$)	Tip Speed Ratio
0	w/o deflector plate	0.312	0.9
	deflector plate at 90°	0.351	0.9
	deflector plate at 45°	0.340	0.9
12.5	w/o deflector plate	0.341	0.9

	deflector plate at 90°	0.364	0.9
	deflector plate at 45°	0.337	0.9
25	w/o deflector plate	0.287	0.9
	deflector plate at 90°	0.344	0.9
	deflector plate at 45°	0.309	0.9

Table 2: Maximum power coefficient (C_p) corresponding to blade twist angle, deflector plate configuration, and tip speed ratio

4.4. Effect of twist angle of blades on the performance of SHK Turbine

Figure 16-18 illustrates variation of coefficient of power (C_p) and coefficient of torque (C_t) with respect to twist angle of blades corresponding to different TSR along with different configuration of deflector plate.

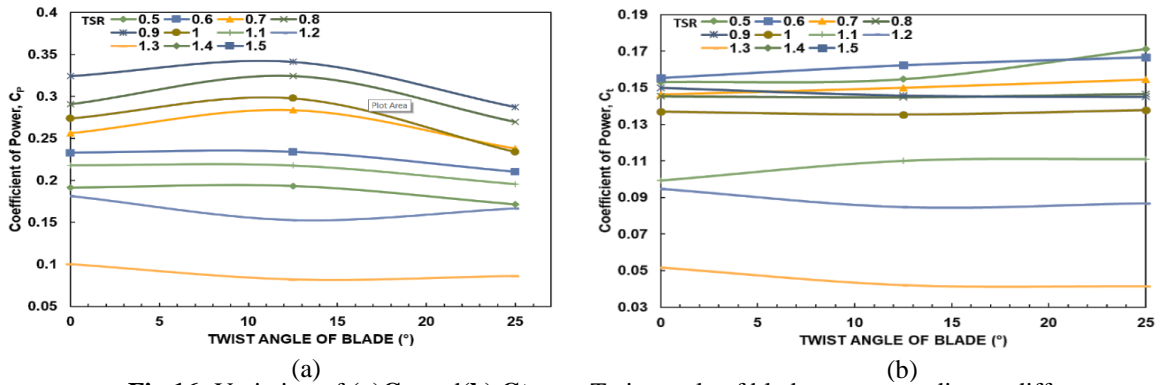


Fig 16: Variation of (a) C_p and (b) C_t w.r.t. Twist angle of blades corresponding to different TSR for turbine without deflector plate

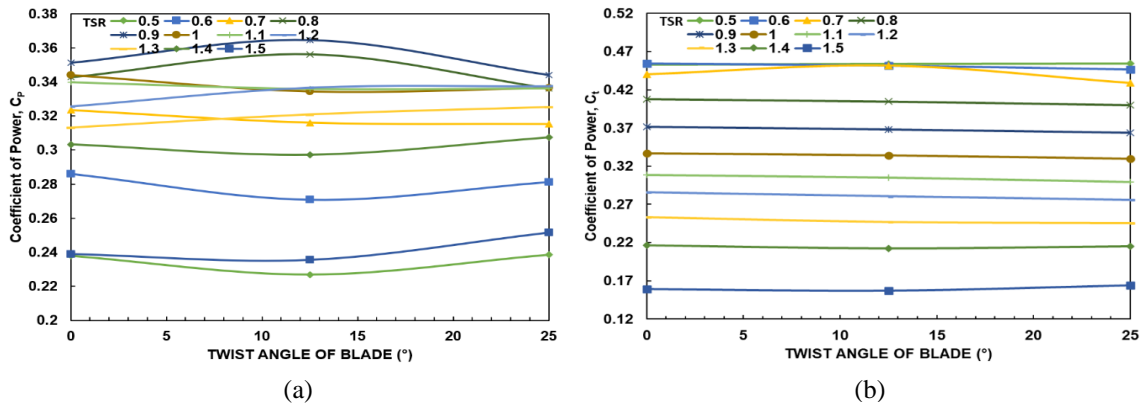
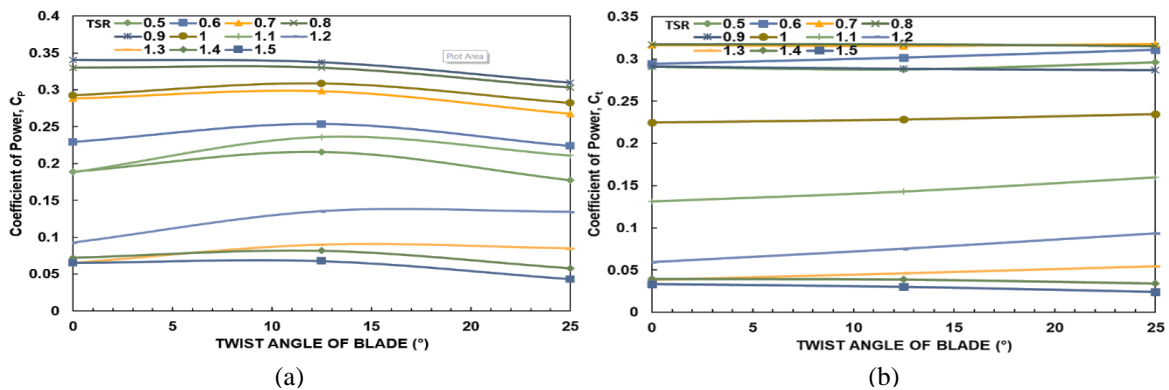


Fig 17: Variation of (a) C_p and (b) C_t w.r.t. twist angle of blades corresponding to different TSR for turbine with deflector plate at 90°



5. Validation

The results for SHK Turbine having twist angle of 0°, 6.25°, 25° with no deflector plate have been validated from Kumar et al. [18]. Tip speed ratio (TSR) considered is 0.9 with free stream velocity of 0.5 m/s. The summarized table is shown below:

Twist Angle (°)	Tip Speed Ratio	V1 (m/s)	Present Study - Coefficient of Power (C _p)	Kumar et al. - Coefficient of Power (C _p)	Error %
0	0.9	0.5	0.312	0.31	0.64
12.5	0.9	0.5	0.341	0.34	0.29
25	0.9	0.5	0.282	0.28	0.71

Table 3: Validation of results obtained in this research

5. Conclusions

According to the simulation findings, the turbine's performance in terms of coefficient of power has a maximum value of C_p of 0.364 at a TSR value of 0.9 at a blade twist angle of 12.5° with deflector plate at 90° and free stream velocity of 0.5 m/s. The highest value of coefficient of torque C_t for the turbine's performance is 0.454 at a TSR value of 0.5 at a blade twist angle of 25° with deflector plate at 90° and free stream velocity of 0.5 m/s. It is observed that as the TSR value increases, coefficient of power (C_p) first increases and afterwards decreases but there is decrease in coefficient of torque (C_t), so it is recommender to keep the TSR in the range of 0.7-0.9 for improved performance of the turbine.

Considering varying C_p with respect to twist angle of blade then we can observe that C_p may increase or decrease based on TSR value and deflector angle (δ). For example, SHK Turbine with deflector plate at 90° shows that for TSR=0.7 the C_p value keeps on decreasing as we increase the twist angle but for TSR=0.8 and TSR=0.9 the C_p value first increases till blade twist angle of 12.5° and thereafter decreases. But for TSR=1 the C_p value first decreases till blade twist angle of 12.5° and thereafter increases as we increase the blade twist angle. It is also observed from the analysis that when TSR is increased above 1.4 then coefficient of torque (C_t) becomes negative which shows inherent unsteady aerodynamic behaviour. So it can be concluded that operating SHT at TSR of above 1.4 is unfavourable.

The current study might be valuable for future research into the performance of Savonius hydrokinetic turbines with various system parameters such as blade shape factor, number of stages, blade arc angle and operating parameter such as blockage ratio and flow velocity and. The scope for further improvisation is still open to further study and development, and will undoubtedly help us meet rising power demand by achieving renewable energy

References

- [1] Loots, I., Van Dijk, M., Barta, B., Van Vuuren, S.J., Bhagwan, J.N. A review of low head hydropower technologies and applications in a South African context. *Renewable and Sustainable Energy Reviews*, 2015;50:1254–68. <https://doi.org/10.1016/j.rser.2015.05.064>.
- [2] World Energy Outlook 2019. OECD; 2019. <https://doi.org/10.1787/caf32f3b-en>.
- [3] International Energy Agency (IEA), CO2 emissions Analysis - Global Energy Review. Paris; 2021.
- [4] International Renewable Energy Agency (IRENA). Renewable Capacity Statistics. Abu Dhabi; 2022.
- [5] Renewables, Renewable Energy Policy Network for the 21st century (2018) - Global Status Report. Paris; 2018.
- [6] Tanbhir, T., Nawshad, U. A., Islam, N., Sina, I., Syfullah, K., & Raiyan, R. (2011). Micro hydro power: promising solution for off-grid renewable energy source. *International Journal of Scientific and Engineering Research*, 2(12), 1–5.
- [7] Khan, M. J., Iqbal, M. T., & Quaicoe, J. E. (2008). River current energy conversion system: progress, prospects and challenges. *Renewable and Sustainable Energy Reviews*, 12, 2177–2193. <https://doi.org/10.1016/j.rser.2007.04.016>.
- [8] Vermaak, H. J., Kusakana, K., & Koko, S. P. (2014). Status of micro-hydrokinetic river technology in rural applications: A review of literature. *Renewable and Sustainable Energy Reviews*, 29, 625–633. <https://doi.org/10.1016/j.rser.2013.08.066>.
- [9] Balat, M. (2006). Hydropower systems and hydropower potential in the European Union countries. *Energy Sources, Part A: Recovery, Utilization and Environmental Effects*, 28 (10): 965-978. <https://doi.org/10.1080/00908310600718833>
- [10] Kamoji, M. A., Kedare, S. B., & Prabhu, S. V. (2008). Experimental investigation on the effect of overlap ratio and blade edge conditions on the performance of conventional Savonius rotor. *Wind Engineering*, 32(2), 163–178.

<https://doi.org/10.1260/030952408784815826>.

- [11] Savonius S. The S-rotor and its applications. *Mechanical Engineering* 1931; 53(5):333-8
- [12] Akwa, J. V., Vielmo, H. A., & Petry, A. P. (2012). A review on the performance of Savonius wind turbines. *Renewable and Sustainable Energy Reviews*, 16(5), 3054–3064. <https://doi.org/10.1016/j.rser.2012.02.056>.
- [13] Altan, B.D., Atilgan, M. (2008). An experimental and numerical study on the improvement of the performance of Savonius wind rotor. *Energy Conversion and Management*; 49(12): 3425-3432. <https://doi.org/10.1016/j.enconman.2008.08.021>
- [14] Wahyudi, B., Soeparman, S., Wahyudi, S., and Denny, W. (2013). A simulation study of Flow and Pressure distribution patterns in and around of Tandem Blade Rotor of Savonius (TBS) Hydrokinetic turbine model. *Journal of Clean Energy Technologies*; 1: 286-291. <https://doi.org/10.7763/JOCET.2013.V1.65>
- [15] Saha, U.K., Rajkumar, M.J. (2006). On the performance analysis of Savonius rotor with twisted blades. *Renewable Energy*; 31(11):1776–88. <https://doi.org/10.1016/j.renene.2005.08.030>
- [16] Akwa JV, Vielmo HA, Petry AP. (2012). A review on the performance of Savonius wind turbines. *Renew Sustain Energy Rev*;16(5):3054–64. <https://doi.org/10.1016/j.rser.2012.02.056>
- [17] Saha UK, Thotla S, Maity D. (2008) Optimum design configuration of Savonius rotor through wind tunnel experiments. *Journal of Wind Engineering and Industrial Aerodynamics*;96(8– 9):1359–75. <https://doi.org/10.1016/j.jweia.2008.03.005>
- [18] Kumar A., Saini R.P., (2017). Performance analysis of a Savonius hydrokinetic turbine having twisted blades. *Renewable Energy*, 108, 502-522. <https://doi.org/10.1016/j.renene.2017.03.006>.
- [19] Pham L. Riverine Hydrokinetic Technology: A Review. Oregon Tech – REE516 Term Paper; 2014.
- [20] Sheldahl RE, Feltz LV, Blackwell BF. (1978). Wind tunnel performance data for two and three-bucket Savonius rotors. *AIAA Journal of Energy*;2(3):160–4. <https://doi.org/10.2514/3.47966>
- [21] Zhao Z, Zheng Y, Xu X, Liu W, Hu G. (2009). Research on the Improvement of the Performance of Savonius Rotor Based on Numerical Study. In: *Proceedings of international conference on sustainable power generation and supply (SUPERGEN)*; p.1–6. <https://doi.org/10.1109/SUPERGEN.2009.5348197>
- [22] Kailash G, Eldho TI, Prabhu SV. (2012). Performance study of modified Savonius water turbine with two deflector plates. *International Journal of Rotating Machinery*, vol., Article ID 679247, p. 12. <http://dx.doi.org/10.1155/2012/679247>.
- [23] Kamoji MA, Kedare SB, Prabhu SV. (2009). Experimental investigations on single stage modified Savonius rotor. *Applied Energy*;86(7–8):1064–73.
- [24] Golecha K, Eldho TI, Prabhu SV. (2011). Influence of the deflector plate on the performance of modified Savonius water turbine. *Applied Energy*; 88:3207–17. <https://doi.org/10.1016/j.apenergy.2011.03.025>
- [25] Golecha, K., Eldho, T.I., Prabhu, S.V. (2012). Performance study of modified savonius water turbine with two deflector plates. *International Journal of Rotating Machinery*, Article ID 679247. <https://doi.org/10.1155/2012/679247>
- [26] Kerikous, E., & Thevenin, D. (2019). Optimal shape of thick blades for a hydraulic Savonius turbine. *Renewable Energy*, 134, 629–638. <https://doi.org/10.1016/j.renene.2018.11.037>.
- [27] Grönman, A., Tianinen, J., & Jaatinen-Värri, A. (2019). Experimental and analytical analysis of vaned Savonius turbine performance under different operating conditions. *Applied Energy*, 250, 864–872. <https://doi.org/10.1016/j.apenergy.2019.05.105>.
- [28] Iio, S., Katayama, Y., Uchiyama, F., Sato, E., & Ikeda, T. (2011). Influence of setting condition on characteristics of Savonius hydraulic turbine with a shield plate. *Journal of Thermal Science*, 20(3), 224–228. <https://doi.org/10.1007/s11630-011-0462-9>
- [29] Bhattacharjee, S., Arora, B. B., & Kashyap, V. (2019). Optimization of Race Car Front Splitter Placement Using CFD (No. 2019-01-5097). *SAE Technical Paper*, 2019-01-5097, <https://doi.org/10.4271/2019-01-5097>
- [30] Mohamed, M.H., Janiga, G., Pap, E., Thévenin, D., (2010). Optimization of Savonius turbines using an obstacle shielding the returning blade. *Renewable Energy*, 35(11), 2618-2626. <https://doi.org/10.1016/j.renene.2010.04.007>
- [31] Singh, H. & Arora, B. (2021). Performance characteristics of flow in annular diffuser using CFD. *International Journal of Turbo & Jet-Engines*, 2021-03, <https://doi.org/10.1515/tjeng-2021-0003>